FOREX Publication
Open Access | Rapid and quality publishing

International Journal of
Electrical and Electronics Research (IJEER)
Research Article | Volume 10, Issue 4 | Pages 1005-1012 | e-ISSN: 2347-470X

An Advanced Artificial Neural Network Energy Management in Standalone PV Systems

Emhamed Alzaroog[1*], Mohsen Ben Ammar[2], Mohamed Ali Zdiri[3] and Hsan Hadj Abdallah[4]
[1]*PhD student, Department of Electrical Engineering, CEM Laboratory, ENIS, University of Sfax, Tunisia*
[2]*Associate Professor, Department of Electrical Engineering, CEM Laboratory, ENIS-University of Sfax, Tunisia*
[3]*Assistant Contractual, Department of Electrical Engineering, CEM Laboratory, ENIS, University of Sfax, Tunisia*
[4]*Professor, Department of Electrical Engineering, CEM Laboratory, ENIS, University of Sfax, Tunisia*

***Correspondence:** Emhamed Alzaroog; ealzarooz@gmail.com

ABSTRACT- With the ever-increasing prevalent power crisis and pollution of the environment, solar power, has attracted greater attention as a new and clean energy source. It provides an alternative solution for isolated sites with an unavailable grid connection. However, it is not without any drawbacks, mainly its intermittent nature, related primarily owing to its reliance on meteorological variables such as the temperature outside and the amount of sunlight. In effect, the PV systems that produced electrical energy could well display an electricity excess or deficit at the loads level, likely to result in system service discontinuity. In this respect, the present paper is designed to provide an intelligent management strategy to PV station owners with a dump load. It can involve serving two customers simultaneously according to the following scenarios: the PV production installation of the customer1 is greater than their required load; however, the customer2's neighboring station does not have enough power to cover its electrical load. This case brings electrical energy from the initial station to make up for the shortfall, and vice versa. Lithium-ion batteries step in the case when the essential electrical power cannot be delivered either by the local station or the neighboring one or to keep the accumulated power excess. If one of the stations (1 or 2) detects a power surplus and the batteries are completely charged, the generated power excess must be redirected to a secondary load, commonly known as the dump load. Relying on the artificial neural network controller, the suggested exchange control is used for two independent PV-battery stations with dump load. The MATLAB/Simulink attained simulation turns out to demonstrate the advanced controller's noticeable performance and effectiveness in managing the standalone PV system's operability in terms of continuous electrical energy delivery flow to the resistive load while reducing power waste and increasing the lithium-ion battery lifespan.

Keywords: Solar energy; PV system; Artificial Neural Network control; Dump load; Lithium-ion batteries; Energy control.

ARTICLE INFORMATION
Author(s): Emhamed Alzaroog, Mohsen Ben Ammar, Mohamed Ali Zdiri and Hsan Hadj Abdallah;
Received: 27/08/2022; **Accepted**: 13/10/2022; **Published**: 20/11/2022;
e-ISSN: 2347-470X;
Paper Id: IJEER220748;
Citation: 10.37391/IJEER.100442
Webpage-link:
https://ijeer.forexjournal.co.in/archive/volume-10/ijeer-100442.html

1. INTRODUCTION

The insertion of distributed renewable energy production technologies such as PV and wind in the power grid is increasing day by day. Even though PV electricity production is heavily influenced by changing weather conditions [1], it requires little upkeep and is clean. The major disadvantage it displays consists mainly in the intermittent character, due to its liability to meteorological data variability [2]. There are two types of PV systems: electrical grid-connected PV systems and standalone PV systems. PV solar systems that are electrical grid-connected are designed to meet the annual total consumption of electricity. Off-grid photovoltaic systems were designed to meet energy requirements immediately [3].

Regarding of standalone PV systems, they are two types: either with or without storage sources. The first type displays the advantage of enabling to reach the necessary energy needs continuously [4]. However, due to the presence of storage sources, it is extremely expensive to maintain. As for the second type, it is rather cheap and does not require considerable maintenance. Indeed, the first type is much more recommended in terms of power consumption continuity. Rather than dealing with insufficient electrical power issues, installation owners frequently choose installations with unusual dimensions. In this regard, the photovoltaic station would assist in producing more electricity than the energy demands anywhere at a given time, especially on sunny days. This additional electrical power supply would be squandered once improperly used or stored.

In this paper, a special scheme is advanced, whereby, neighboring off-grid electric installations can be connected to a micro-grid to exchange the excess electric power. In this electrical micro-grid, the generating electric installation could transfer the surplus of output energy to other nearby-based electric installations that were running low on energy on meeting their energy loads. The available energy excess produced will be either stored in the batteries or supplied to the dump load. This dump load is used as an additional load in order to avoid power losses. Accordingly, no loss of energy would be perceived, while the system keeps maintaining its operation in a normal way. Dubbed Simulink, the proposed model includes

FOREX Publication
Open Access | Rapid and quality publishing
International Journal of Electrical and Electronics Research (IJEER)
Research Article | Volume 10, Issue 4 | Pages 1005-1012 | e-ISSN: 2347-470X

all of the standalone PV system relevant components, namely, an MPPT algorithm-driven PV station, a boost converter, lithium-ion batteries, station loads, and dump load.

In effect, to stay balanced through the electrical energy generated and the station-load energy requirements, an efficient energy management algorithm is suggested. This management algorithm should decide on the source wherefrom the PV installation meets its load's energy needs: whether from a located installation, batteries, or having to borrow energy from another neighboring installation. *Figure 1*, below, illustrates the use of two based PV stations with dump load, as depicted in this study. Once sufficient energy is provided, every PV station turns to supply its load. In the power outage event, both stations and the batteries step in to help. It is worth underlining that K_1, K_2, K_{12}, K_{21}, K_{1D}, and K_{2D} denote the IGBT switches applied.

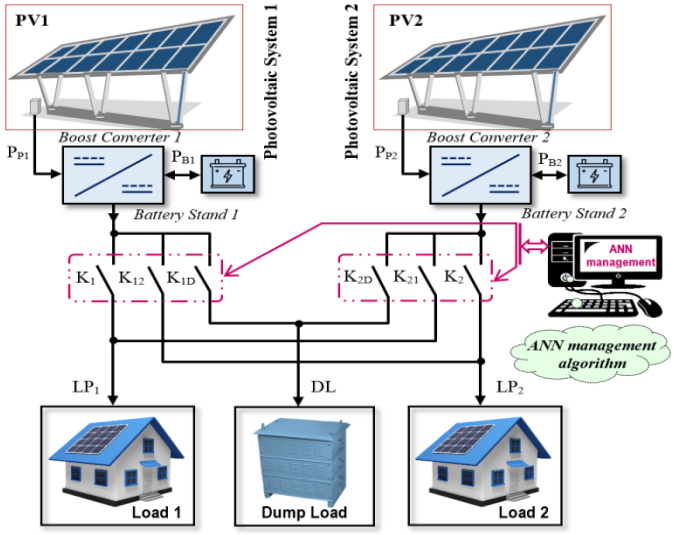

Figure 1: Dual stand-alone photovoltaic systems with dump load

The ANN (artificial neural network) and FLC (fuzzy logic controller) are widely applied for a wide range of complex applications. They can be used to control the voltage-based electric grid, as well as the current and heat cable parameters [5-6]. The FLC demonstrated good accuracy in the command of a bidirectional total power charger, which shall allow both charging and providing vehicle energy to the grid (V2G) [7]. It (FLC) aids in the automatic determination of micro-wave oven cooking time based on quantity and food type [8]. It's also utilized in hybrid power system applications, such as renewable energy with and without storage [9-10]. An adaptive fuzzy logic-based EMS (energy management strategy) for HESS (hybrid energy system storage) in electric vehicle applications is presented in [11]. The proposed system of control employs a multi-agent-based approach that is difficult to create and necessitates extensive computational sources. The ANN controller is also used for HESS control ends. In [12], the adaptive ANN-based management for hybrid AC/DC microgrids is advanced. Accordingly, ANN-based management is used to monitor the maximum power generated by a renewable source and transfer power to the grid. The method relies on an online highly trained neural network control algorithm that is too complex to design and necessitates a lot of computational power to find the best control parameters.
Regarding the present paper, an ANN strategy is designed and adapted for implementation in a standalone hybrid PV system, for the purpose of maximizing the battery lifetime and ensuring power continuity [13-14]. Worth highlighting, in this context, is that the ANN controller exhibits a number of remarkable advantages, mainly: the ability to work with insufficient knowledge; good fault tolerance; the ability to train machines; gradual corruption, and higher robustness. Relying on the ANN controller, the suggested control is employed for two independent PV battery stations with dump load. The simulation results based on MATLAB/Simulink turn out to demonstrate the advanced controller's noticeable performance and effectiveness in terms of continuous power delivery flow to the load while trying to minimize power waste and increase the lithium-ion battery lifetime by reducing the discharge cycle.

The following is how this work is organized. *Section 2* depicts the standalone PV system's main components. *Section 3* enumerates the envisioned ANN-involved steps. *Section 4* highlights the management planning relevant analysis via ANN controller. *Section 5* outlines the simulation attained results with regard to the performance and effectiveness of the advanced ANN controller. As the concluding remarks, they make the subject of *Section 6*.

2. PV POWER SYSTEM ARCHITECTURE

A stand-alone PV installation has been widely applied in distinct areas once no electrical power grid is applied. An Off-grid PV system incorporates photovoltaic panels, an MPPT control, a boost converter, a buck-boost converter, a PID controller, and batteries [15]. The entire dump-load incorporating PV systems were made using MATLAB/Simulink environment, as illustrated in *figure 2*.

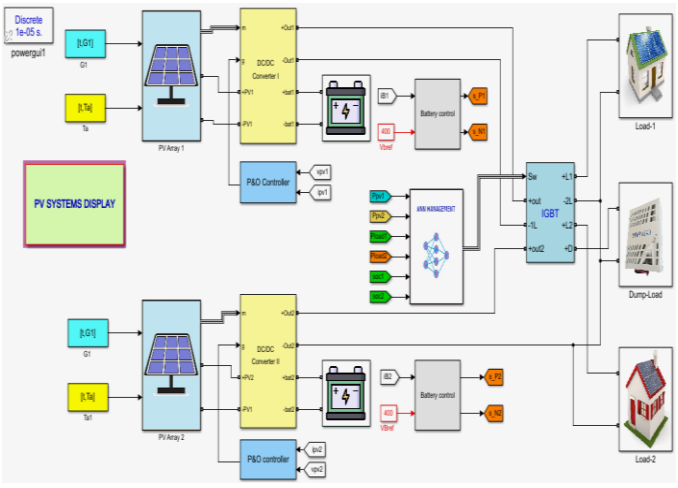

Figure 2: Dual standalone PV systems' ANN energy management Simulink model

2.1 PV Panel

The photovoltaic panels convert electricity from sunlight. A PV generator can be built by linking numerous PV modules in parallel and series [16]. The PV generator is, in fact, a nonlinear

FOREX Publication
Open Access | Rapid and quality publishing
International Journal of Electrical and Electronics Research (IJEER)
Research Article | Volume 10, Issue 4 | Pages 1005-1012 | e-ISSN: 2347-470X

system, as illustrated in *figure 3* below, with an equivalent cell circuit.

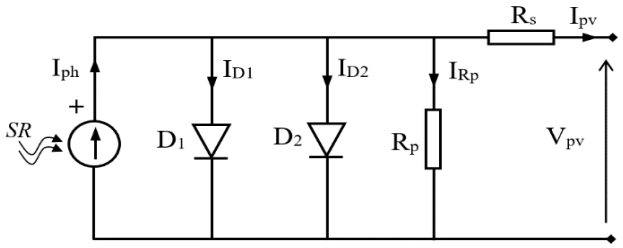

Figure 3: A PV solar cell's equivalent electrical circuit

Several mathematical models' is suggested to describe the semiconductor junctions provided non-linear behavior. The most widely recognized of these models is the 'Four-Parameter Model'. The mono-crystalline and poly-crystalline PV arrays' efficiency is exhaustively investigated in [17-20]. The I_{pv} current can be calculated based on the voltage of the PV array V_{pv}, as follows [21]:

$$I_{pv} = I_{sc}\{1 - F_{11}[exp(F_{22}V_{pv}^{m}) - 1]\} \quad (1)$$

Where F_{11}= *0.01175*, $F_{22}=F_{44}/V_{oc}^{m}$, F_{33}= $ln[(I_{sc}(1+F_{11})-I_{mpp})/(F_{11}\ I_{sc})]$, $F_{44}=ln[(1+F_{11})/F_{11}]$ and m= $ln[F_{33}/F_{44}]/ln[V_{mpp}/V_{oc}]$. V_{mpp} and I_{mpp} denote the PV voltage and current at MPP, respectively. The OCV (open-circuit voltage) and SCC (short-circuit current) are designated by V_{oc} and I_{sc}. The climatic conditions have a noticeable impact on the PV systems. The following equations are useful for processing the *equation (1)* adaptation to meteorological data variations:

$$T_c = T_a + (NOCT - T_0)\frac{G}{G_0} \quad (2)$$

$$\Delta T_C = T_C - T_0 \quad (3)$$

$$\Delta I_{pv} = \alpha\ \frac{G}{G_0}\Delta T_C + \left(\frac{G}{G_0} - 1\right) I_{sc} \quad (4)$$

$$\Delta V_{pv} = -\beta\ \Delta T_C - R_s \Delta I_{pv} = \frac{ln[F_{33}/F_{44}]}{ln[V_{mpp}/V_{oc}]} \quad (5)$$

Where T_0 and G_0 respectively designate the cell temperature and irradiation at STC. T_c and G denote the temperature and irradiation, respectively, of the PV cell. T_a stands for the ambient temperature of the PV cell. A and β are abbreviations for the SCC and OCV temperature coefficients, respectively. R_s designates the serial resistance.

Equations (6) and (7) illustrate the new PV current and voltage expressions, which are as follows:

$$V_{pv,new} = V_{pv} + \Delta V_{pv} \quad (6)$$

$$I_{pv,new} = I_{pv} + \Delta I_{pv} \quad (7)$$

The PV generator is constructed by linking solar PV modules in series (N_{SS}) and parallel (N_{PP}), as presented by [22-23]:

$$P_{pv} = N_{SS}V_{pv}N_{PP}I_{pv} \quad (8)$$

The parameters of the solar panel ADVANCE POWER API-M255 are depicted in the following *table 1*.

Table 1: The API-M255 Module Characteristics

ADVANCE POWER API-M255	
P_{max}	255.51 W
V_{mpp}	30.6 V
I_{mpp}	8.35 A
V_{oc}	37.68 V
I_{sc}	8.67 A
R_S	0.3004 Ω
R_P	1773. 68 Ω
N_{cell}	60

2.2 Description of the MPPT Technique

Various techniques have been employed to monitor the MPP maximum power point. The most widely applied of these techniques are incremental conductance, fractional OCV, fractional SCC, perturb and observe (hill-climbing technique), neural network, and fuzzy logic control [24-33]. Regarding the present study, the FLC is used as the MPPT technique. The FLC maintains command of the photovoltaic system based on a data knowledge process. The FLC relevant stages are categorized as:

(1) Fuzzification (2) Decision making and (3) Defuzzification; The FLC block structure is depicted in *figure 4*, below.

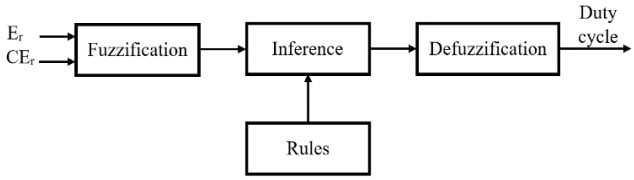

Figure 4: Block diagram of the FLC

The FLC inputs, output, and duty cycle, respectively referred to as E_r and CE_r are provided by:

$$\begin{cases} E_r = \dfrac{P_{pv}(K) - P_{pv}(K-1)}{V_{pv}(K) - V_{pv}(K-1)} \\ CE_r = E_r(K) - E_r(K-1) \end{cases} \quad (9)$$

2.3 Converter Modelling

The converter in use is a setup voltage converter that is controlled via PWM. The PWM bloc's input is generated using MPPT techniques [34]. *Figure 5* depicts the boost converter, which contains an inductor, a diode, a high-frequency switch, and a capacitor [35-36]. The voltage of the boost converter can be depicted in accordance with two modes of operation: passing and blocking, as figured in *equations (10) and (11)* [37], below:

FOREX Publication
Open Access | Rapid and quality publishing
International Journal of Electrical and Electronics Research (IJEER)
Research Article | Volume 10, Issue 4 | Pages 1005-1012 | e-ISSN: 2347-470X

$$\frac{di_L}{dt} = \frac{1}{L}[V_{in} - V_{out}(1-D)] \quad (10)$$

$$\frac{dV_{out}}{dt} = \frac{1}{C_1}[i_L(1-D) - I_{out}] \quad (11)$$

With: L represents the inductance value (in H), i_L denotes the inductor current, C_1 designates the capacitance of the input (in F) and I_{out} denotes the load current.

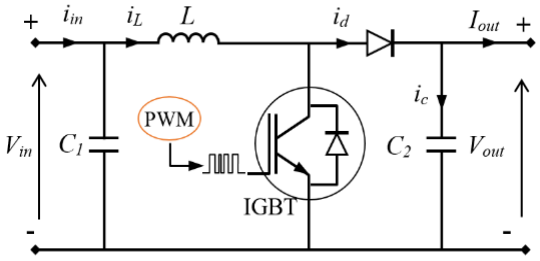

Figure 5: Equivalent circuit model of the boost converter

2.4 Battery Modelling

To model the lithium-ion battery, MATLAB/Simulink is used. *Figure 6* depicts the fractional order of the ECM. It is utilized to keep an optimal general pattern among ECMs by reducing the computational burden and improving the efficiency of outmoded existing ECM failings. The SOC of a lithium-ion battery measures the quantity of useable energy during the current cycle, as defined by:

$$SOC(t) = SOC(t0) - \frac{\int_{t0}^{t} I_B(\tau)d\tau}{Q_C} \quad (12)$$

With: I_B is the current, *t0* represents the initial time, and Q_C denotes the nominal capacity.

In the following equation, we presented a somewhat different link between cycle-life and DOD (1-SOC):

$$N = N_{80} * DOD' * e^{(£*(1-DOD'))} \quad (13)$$

Wherein N_{80} seems to be the cycle life at DOD = 80 %, and £ denotes a constant with values between 2.25 and 3.

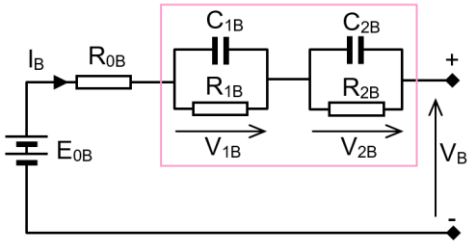

Figure 6: Lithium-ion battery model

Using the ECM as presented in *Figure 6*, the terminal voltage V_B turns out to be determined using the formula below:

$$V_B(t) = E_0(SOC) - I_B(t)R - C(t) \quad (14)$$

With: R denotes the internal resistance and $C(t)$is a correction factor resulting from the model's lack of accuracy and environmental factors [38]. The ECM with a 2-RC circuit is used to strike a compromise among both computation complexity and precision, where:

$$\dot{V}_1(t) = -\frac{V_{1B}(t)}{R_{1B}C_{1B}} + \frac{I_B(t)}{C_{1B}} \quad (15)$$

$$\dot{V}_2(t) = -\frac{V_{2B}(t)}{R_{2B}C_{2B}} + \frac{I_B(t)}{C_{2B}} \quad (16)$$

With: R_{1B}, R_{2B}, and C_{1B}, C_{2B} respectively designate the RC network diffusion resistances and diffusion capacitances. These parameters can be calculated along with the ohmic resistance using the technique of fitting exponential functions or a straightforward least squares algorithm [39]. Each station's battery (PV station 1 or 2) is monitored by a buck-boost converter, which is controlled by a discrete PID controller. The model of the PID controller Simulink is highlighted in *figure 7*. Accordingly, the upper switch *Sp1* charges the battery, while the bottom switch *Sn1* discharges it.

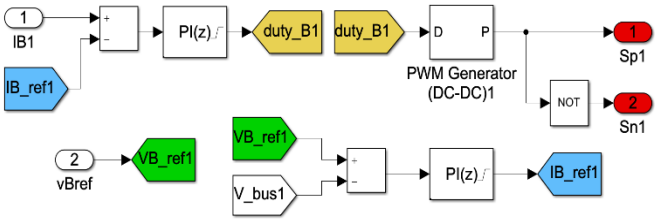

Figure 7: Simulink model of the PID controller

3. ANN CONTROL ALGORITHM

More recently, the ANN technique has attracted great interest in the PV systems MPP and energy management control tracking process [40]. It is worth underlining that the proposed technique relies heavily on the ANN to ensure an effective resolution of complex problems. The neural network architecture is made up of the input, hidden, and output layers. A neuron (also known as a node) is linked between multi-layer networks with each layer of the network [41-43]. The ANN technique entails two critical stages: training and operation. The neural network model's inputs and outputs are, respectively: P_{P1}, P_{P2}, LP_1, LP_2, SOC_1, SOC_2, and K_1, K_2, K_{12}, K_{21}, K_{1D}, and K_{2D}, as illustrated in *figure 8*.

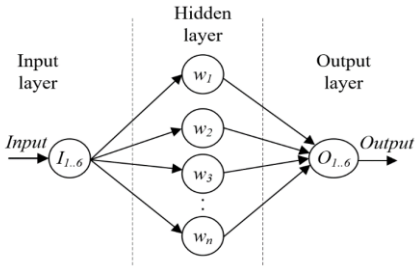

Figure 8: ANN block diagram

Where P_{P1} designates the first station's respective power, and P_{P2} is the second station's respective power. In addition, $\Delta P_{P1}LP_1$ and $\Delta P_{P2}LP_2$ can be formulated as follows:

FOREX Publication
Open Access | Rapid and quality publishing
International Journal of Electrical and Electronics Research (IJEER)
Research Article | Volume 10, Issue 4 | Pages 1005-1012 | e-ISSN: 2347-470X

$$\Delta P_{P1}LP_1 = P_{P1} - LP_1 \quad (17)$$

$$\Delta P_{P2}LP_2 = P_{P2} - LP_2 \quad (18)$$

In order to train the Levenberg-Marquardt algorithm, a set of switch-state data points that were already taken from the Simulink simulation were used. The training performance curve in *figure 9* shows that the MSE error has fallen to 0.00073647 after 109 epochs.

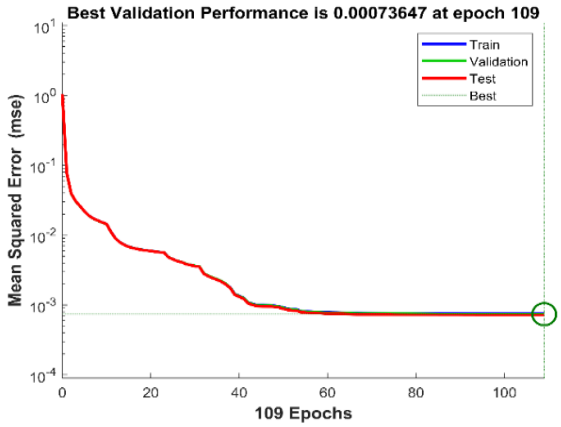

Figure 9: Artificial Neural Network performances

4. MANAGEMENT PLANNING VIA ANN

To cover the stations' loads, our designed system should be able to decide whether to connect two standalone photovoltaic stations with a dump load. As shown in *figure 10*, clear criteria have been followed to ensure an efficient management algorithm.

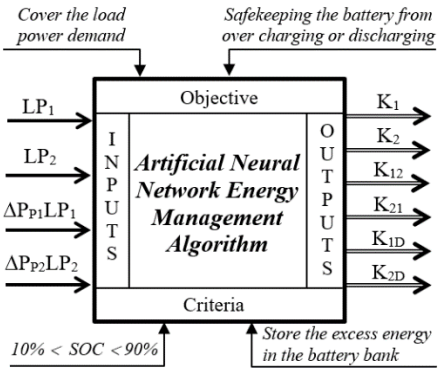

Figure 10: The proposed management strategy schemes

While complying with the criteria mentioned, the power control algorithm has been implemented through the use of an ANN technique. The management algorithm involves four operating modes as presented in the following figure.

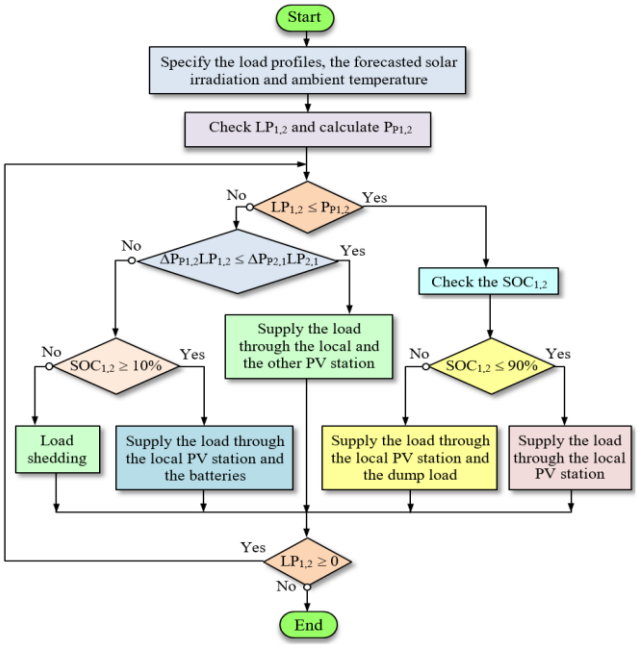

Figure 11: The advanced energy management organogram

The following *table* illustrates the switches states considering the climatic condition and load variations:

Table 2: Switches states

Modes	K_1	K_2	K_{12}	K_{21}	K_{1D}	K_{2D}
$LP_1 \leq P_{P1}$ *and* $SOC_1 \leq 90\ \%$	1	0	0	0	0	0
$LP_2 \leq P_{P2}$ *and* $SOC_2 \leq 90\ \%$	0	1	0	0	0	0
$LP_1 \leq P_{P1}$ *and* $SOC_1 \geq 90\ \%$	1	0	0	0	1	0
$LP_2 \leq P_{P2}$ *and* $SOC_2 \geq 90\ \%$	0	1	0	0	0	1
$LP_1 \geq P_{P1}$ *and* $\Delta PL_1 \leq \Delta PL_2$	1	0	0	1	0	0
$LP_2 \geq P_{P2}$ *and* $\Delta PL_2 \leq \Delta PL_1$	0	1	1	0	0	0

5. SIMULATION RESULTS

The system mathematical model, which mainly depends on, can be used to calculate the generated PV power. *Figure 12* depicts the real *G* and *T* meteorological data.

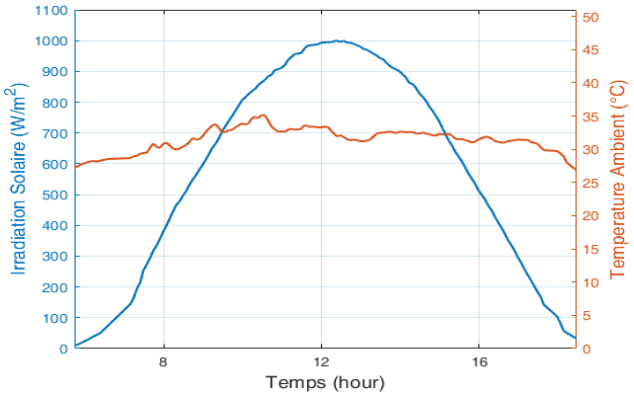

Figure 12: The (G and T) meteorological database

FOREX Publication
Open Access | Rapid and quality publishing
International Journal of Electrical and Electronics Research (IJEER)
Research Article | Volume 10, Issue 4 | Pages 1005-1012 | e-ISSN: 2347-470X

The PV system parameters are illustrated in the following *table*. Application of the advanced ANN controller for loads (1 and 2) and dump load describes the switchers' state as illustrated in *figure 13* and *figure 14*.

Under the climatic conditions and load variations, it is clear that the neighboring station intervenes once the PV station isn't able to maintain the entire load requirements. Furthermore, the first PV station intervenes to supply the dump load with energy in the case of power excess, and both of the PV stations' batteries are fully charged. Furthermore, the battery can contribute to meeting the power needs of the load and storing the excess energy depending on its charge state.

Table 3: PV systems parameters

PV1 generators' parameters	
P_{max}	5110.2 W
V_{mpp}	153 V
I_{mpp}	33.4 A
PV2 generators' parameters	
P_{max}	6387.75 W
V_{mpp}	153 V
I_{mpp}	41.75 A
DC/DC converters parameters	
C_1	440 µF
C_2	3000 µF
L	47 µH
Lithium-ion battery parameters	
V_B	220 V
C_B	50 Ah
Dump load parameter	
P_{DL}	800 W

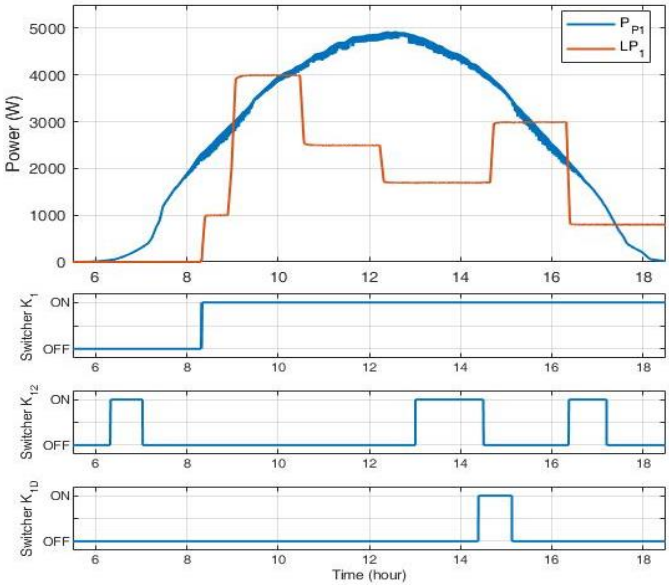

Figure 13: The PV power, the load power of the first station, and the state switches of K_1, K_{12}, and K_{1D}

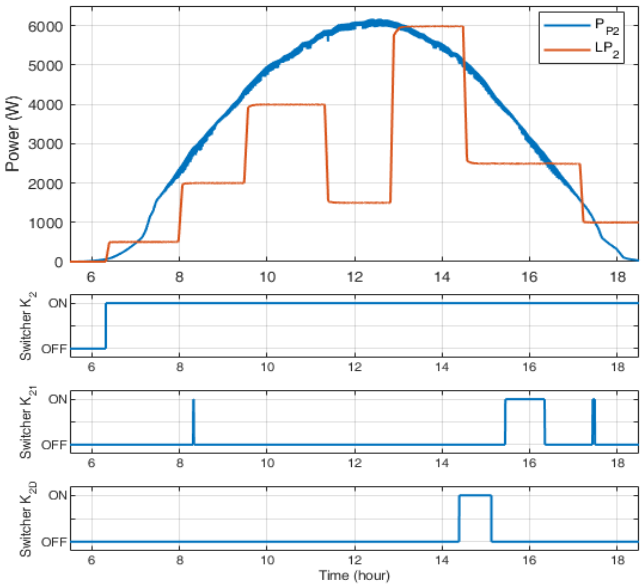

Figure 14: The second station's PV power and load power and the state switches of K_2, K_{21} and K_{2D}

Figure 15 shows the battery reference voltage and measurement voltage for the initial station. Depending on this figure, the DC bus voltage remains constantly equal to 400 V during the variations of the climatic condition, thus, maintaining the continuous bus-voltage fluctuationality rate at a relatively acceptable level. It does not seem to affect the accuracy of the investigated strategy.

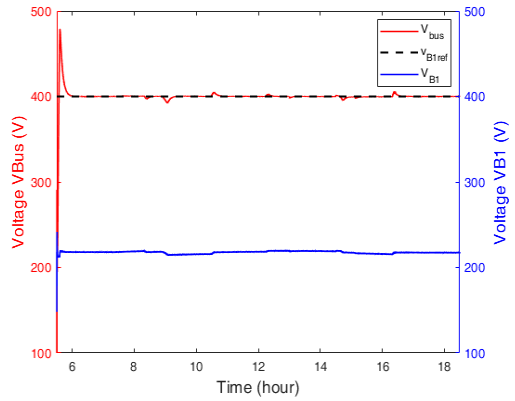

Figure 15: The first battery reference and measurement voltage

The percentage of the power provided to load 1 from the PV1 station (P_{K1}) and dump load (P_{K1D}), the power provided to load 1 from the PV2 station (P_{K21}), and the battery power levels' percentages are presented in figure 16. Accordingly, 81 % of the first load power is drawn from the local PV installation (P_{K1}), 14 % is drawn from the neighboring photovoltaic installation (P_{K21}), and 7 % from the first battery bank (P_{B1}). Furthermore, 3 % of the dump load level is drawn from the first PV installation. The percentage of power provided to load 2 from PV2 station (P_{K2}) and dump load (P_{K2D}), the power provided to load 2 from PV1 station (P_{K12}), and the battery power percentage levels are illustrated in *figure 16*. Accordingly, 73 % of the load's total energy is drawn from the

FOREX Publication
Open Access | Rapid and quality publishing
International Journal of Electrical and Electronics Research (IJEER)
Research Article | Volume 10, Issue 4 | Pages 1005-1012 | e-ISSN: 2347-470X

local installation (P_{K2}), 9 % is drawn from the neighboring photovoltaic installation (P_{K12}), and 9 % from the battery power bank (PB2). Besides, 5 % of the dump load energy is drawn from the second PV installation.

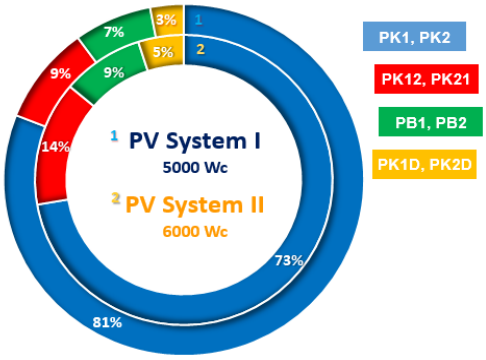

Figure 16: Powers exchanged to feed load 1, load 2, and dump load

6. CONCLUSION

The stand-alone electrical PV system has been typically utilized in remote locations, in which the power grid is generally unavailable. Unless the power necessary to supply the electrical load does not exist, the latter will automatically disconnect. In this paper, a new strategy is developed, whereby, energy is shared between standalone storage-system equipped PV systems and dump load mutual contribution. Accordingly, MATLAB/Simulink was used to design two standalone PV stations with dump load. The model of Simulink includes a whole of the PV installation's necessary components: PV panels employing the FLC technique type, a boost converter, a bidirectional converter, batteries, loads, and a dump load. Due to the standalone PV system's reliance on renewable energy sources, electrical energy management becomes rather complex. Accordingly, an effective electrical energy management algorithm involving two standalone PV systems with dump load has been advanced considering the variations of the climatic conditions and loads. Regarding the load requirements feeding process, the proposed controller is designed in such a way as to deploy the ANN controller. The developed ANN controller achieved simulation results turn out to testify to the model's remarkable efficiency in matters of power management, whether with regard to maintaining service and preventing electrical power losses. In congruence with these findings, the new design's significant performance and perceived supremacy in regard to energy exchange between two PV stations are highly noticeable.

REFERENCES

[1] Manandhar, U.; Ukil, A.; Gooi, H. B.; Tummuru, N. R.; Kollimalla, S. K.; Wang, B.; Chaudhari, K. Energy management and control for grid connected hybrid energy storage system under different operating modes. IEEE Transactions on Smart Grid 2017, 10, 1626-1636.

[2] Thiam, D. R.; Renewable decentralized in developing countries: an appraisal from microgrids project in Senegal. Renewable Energy 2010, 35, 1615–1623.

[3] Rajani, V.; Pandya, V.; Suvariya, A. A Real-Time Comparison of Standalone and Grid Connected Solar Photovoltaic Generation Systems. International Journal of Energy and Power Engineering 2015, 9, 1000-1007.

[4] Perea-Moreno, A. J.; Hernandez-Escobedo, Q.; Garrido, J.; Verdugo-Diaz, J. D. Stand-Alone Photovoltaic System Assessment in Warmer Urban Areas in Mexico. Energies 2018, 11, 284-296.

[5] Kurniawan, A. C.; Afandi, A. N.; Sendari, S.; Wibawa, A. P.; Fadlika, I. Application of Fuzzy Logic to Electrical Protection Devices. Int. Journal of Physics: Conference Series 2020, 1501, 012013.

[6] Zdiri, M. A.; Khelifi, B.; Salem, F. B.; Abdallah, H. H. A Comparative Study of Distinct Advanced MPPT Algorithms for a PV Boost Converter. International Journal of Renewable Energy Research (IJRER) 2021, 11, 1156-1165.

[7] V. Raju and S. P. Phung, "Economic dimensions of blockchain technology: In the context of extention of cryptocurrencies," Int. J. Psychosoc. Rehabil., vol. 24, no. 2, pp. 29–39, Feb. 2020, doi: 10.37200/IJPR/V24I2/PR200307.

[8] Lynn, N. D.; Sourav, A. I.; Santoso, A. J. A Fuzzy Logic-based Control System for Microwave Ovens. Int. Journal of Physics: Conference Series 2020, 1577, 012021.

[9] Feddaoui, O.; Toufouti, R.; Jamel, L.; Meziane, S. Fuzzy logic control of hybrid systems including renewable energy in microgrids. International Journal of Electrical & Computer Engineering 2020, 10, 5559-5569.

[10] M. R. H. Polas, V. Raju, S. M. Hossen, A. M. Karim, and M. I. Tabash, "Customer's revisit intention: Empirical evidence on Gen-Z from Bangladesh towards halal restaurants," J. Public Aff., 2020, doi: 10.1002/PA.2572.

[11] Yin, H.; Zhou, W.; Li, M.; Ma, C.; Zhao, C. An adaptive fuzzy logic-based energy management strategy on battery/ultracapacitor hybrid electric vehicles. IEEE Trans. Transport. Electrific. 2016, 2, 300–311.

[12] Chettibi, N.; Mellit, A.; Sulligoi, G.; Pavan, A. M. Adaptive neural network-based control of a hybrid AC/DC microgrid. IEEE Trans. Smart. Grid 2016, 9, 1667-1679.

[13] V. Raju, "Implementing Flexible Systems in Doctoral Viva Defense Through Virtual Mechanism," Glob. J. Flex. Syst. Manag., vol. 22, no. 2, pp. 127–139, Jun. 2021, doi: 10.1007/S40171-021-00264-Y.

[14] Javed, K.; Ashfaq, H.; Singh, R.; Hussain, S. M.; Ustun, T. S. Design and performance analysis of a stand-alone PV system with hybrid energy storage for rural India. Electronics 2019, 8, 952.

[15] Bonkile, M. P.; Ramadesigan, V. Power management control strategy using physics-based battery models in standalone PV-battery hybrid systems. Journal of Energy Storage 2019, 23, 258-268.

[16] Babalola, O. S.; Komolafe, O. A.; Jegede, O. O.; Ayoola, M. A. Photovoltaic Generating System Parameter Sizing for Building. Journal of Energy Technologies and Policy 2014, 4, 65-73.

[17] Khezzar, R.; Zereg, M.; Khezzar, A. Modeling improvement of the four parameter model for photovoltaic modules. Solar Energy 2014, 110, 452-462.

[18] Chenni, R.; Makhlouf, M.; Kerbache T.; Bouzid, A. A detailed modeling method for photovoltaic cells. Energy 2007, 32, 1724-1730.

[19] Li, Q.; Zhao, S.; Wang, M.; Zou, Z.; Wang B.;and Chen, Q. An improved perturbation and observation maximum power point tracking algorithm based on a PV module four-parameter model for higher efficiency. Applied Energy 2017, 195, 523-537.

[20] Li, S. A maximum power point tracking method with variable weather parameters based on input resistance for photovoltaic system. Energy Conversion and Management 2015, 106, 290–299.

[21] Lalouni, S.; Rekioua, D.; Rekioua, T.; Matagne, E. Fuzzy logic control of stand-alone photovoltaic system with battery storage. Journal of power Sources 2009, 193, 899-907.

[22] Ammar, R. B.; Ammar, M. B.; Oualha, A. Photovoltaic power forecast using empirical models and artificial intelligence approaches for water pumping systems. Renewable Energy 2020, 153, 1016-1028.

[23] Ammar, M. B.; Ammar, R. B.; and Oualha, A. Photovoltaic power prediction for solar car park lighting office energy management. Journal of Energy Resources Technology 2020, 143, 1-11.

[24] Gomathy, S.; Saravanan, S.; Thangavel, S. Design and implementation of maximum power point tracking (MPPT) algorithm for a standalone PV

International Journal of Electrical and Electronics Research (IJEER)
Research Article | Volume 10, Issue 4 | Pages 1005-1012 | e-ISSN: 2347-470X

system. International Journal of Scientific & Engineering Research 2012, 3, 1-7.

[25] Bouchafaa, F.; Hamzaoui, I.; Hadjammar, A. Fuzzy Logic Control for the tracking of maximum power point of a PV system. Energy Procedia 2011, 6, 633-642.

[26] Pakkiraiah, B.; Sukumar, G. D. Research survey on various MPPT performance issues to improve the solar PV system efficiency. Journal of Solar Energy 2016, 2016, 1-20.

[27] Baba, A. O.; Liu, G.; Chen, X. Classification and Evaluation Review of Maximum Power Point Tracking Methods. Sustainable Futures 2020, 2, 100020.

[28] Fathabadi, H. Novel standalone hybrid solar/wind/fuel cell/battery power generation system. Energy 2017, 140, 454-465.

[29] Nusaif, A. I.; Mahmood, A. L. MPPT Algorithms (PSO, FA, and MFA) for PV System Under Partial Shading Condition, Case Study: BTS in Algazalia, Baghdad. International Journal of Smart Grid-ijSmartGrid 2020, 4, 100-110.

[30] Belkaid, A.; Colak, I.; Kayisli, K.; Bayindir, R. Design and implementation of a cuk converter controlled by a direct duty cycle INC-MPPT in PV battery system. International Journal of Smart Grid-ijSmartGrid 2019, 3, 19-25.

[31] Belkaid, A.; COLAK, I.; KAYISLI, K.; BAYINDIR, R. Improving PV System Performance using High Efficiency Fuzzy Logic Control. 8th International Conference on Smart Grid (icSmartGrid) 2022, 152-156.

[32] Himabindu Eluri; M. Gopichand Naik. Energy Management System and Enhancement of Power Quality with Grid Integrated MicroGrid using Fuzzy Logic Controller. IJEER 2022, 10(2), 256-263.

[33] Srivastava, Spandan, et al. Comparative Analysis of Particle Swarm Optimization and Artificial Neural Network Based MPPT with Variable Irradiance and Load. IJEER 2022, 10(3), 460-465.

[34] Zdiri, M. A.; Ben Ammar, M.; Bouzidi, B.; Abdelhamid, R.; Abdallah, H. H. An advanced switch failure diagnosis method and fault tolerant strategy in photovoltaic boost converter. Electric Power Components and Systems 2020, 48, 1932-1944.

[35] Martinez, W.; Imaoka, J.; Yamamoto, M.; Umetani, K. High step-up interleaved converter for renewable energy and automotive applications. International Conference on Renewable Energy Research and Applications (ICRERA) 2015, 809-814.

[36] V. Raju and S. P. Phung, "Production of methane gas from cow's residue: Biogas as alternative energy in transportation and electricity," Eurasian J. Anal. Chem., vol. 13, no. 6, pp. 121–124, 2018.

[37] Zebraoui, O.; Bouzi, M. Improved MPPT controls for a standalone PV/wind/battery hybrid energy system. International Journal of Power Electronics and Drive Systems 2020, 11, 988-1001.

[38] Chen, X.; Shen, W.; Cao, Z.; Kapoor, A. A novel approach for state of charge estimation based on adaptive switching gain sliding mode observer in electric vehicles. Journal of Power Sources 2014, 246, 667–678.

[39] Waag, W.; Kabitz, S.; Sauer, D.U. Experimental investigation of the lithium-ion battery impedance characteristic at various conditions and aging states and its influence on the application. Applied Energy 2003, 102, 885–897.

[40] Zdiri, M. A.; Guesmi, T.; Alshammari, B. M.; Alqunun, K.; Almalaq, A.; Salem, F. B.; Toumi, A. Design and Analysis of Sliding-Mode Artificial Neural Network Control Strategy for Hybrid PV-Battery-Supercapacitor System. Energies 2022, 15, 4099.

[41] M. R. H. Polas, V. Raju, M. Muhibbullah, and M. I. Tabash, "Rural women characteristics and sustainable entrepreneurial intention: a road to economic growth in Bangladesh," J. Enterprising Communities, vol. 16, no. 3, pp. 421–449, May 2022, doi: 10.1108/JEC-10-2020-0183.

[42] Roumpakias, E.; Stamatelos, T. Prediction of a Grid-Connected Photovoltaic Park's Output with Artificial Neural Networks Trained by Actual Performance Data. Appl. Sci. 2022, 12, 6458.

[43] Jaber, M.; Abd Hamid, A. S.; Sopian, K.; Fazlizan, A.; Ibrahim, A. Prediction Model for the Performance of Different PV Modules Using Artificial Neural Networks. Appl. Sci. 2022, 12, 3349.